

# Bone Remodeling Changes in an Individual with Tuberculosis-Induced, Left-Sided Femoroacetabular Joint Destruction, from Nineteenth-Century Milton, New Zealand

Anne Marie E. Snoddy,<sup>a,\*^</sup> Justyna J. Miskiewicz,<sup>b,c,\*^</sup> Karen M. Cooke,<sup>b</sup> Peter Petchey,<sup>d</sup> and Hallie R. Buckley<sup>a</sup>

<sup>a</sup>Department of Anatomy, University of Otago, Dunedin, Otago, New Zealand

<sup>b</sup>School of Archaeology and Anthropology, Australian National University, Canberra, Australian Capital Territory, Australia

<sup>c</sup>School of Social Science, University of Queensland, St Lucia, Queensland, Australia

<sup>d</sup>Archaeology Programme, School of Social Sciences, University of Otago, Otago, New Zealand

\*Joint first authors

<sup>^</sup>Correspondence to: Anne Marie E. Snoddy, University of Otago, Department of Anatomy, 270 Great King Street, Dunedin, Otago 9018, New Zealand; and Justyna J. Miskiewicz, 44 Linnaeus Way, Canberra, ACT 0200, Australia

e-mail: annie.sohler@otago.ac.nz; justyna.miskiewicz@anu.edu.au

## ABSTRACT

Bone is dynamic, undergoing metabolic changes in response to behavioral and pathological stimuli. This information can be reconstructed in bioarchaeology using histological methods, providing another avenue to explore the experiences of past peoples. We report histological findings from midshaft femoral cortical bone of an identified individual from nineteenth-century New Zealand, who suffered from tuberculosis and had a historically documented period of invalidism. *Materials:* Burial 21 (B21) is a middle-aged male excavated from the nineteenth-century site of St. John's burial ground, Milton. B21's left proximal femur and acetabulum exhibited lytic lesions associated with tuberculosis-induced destruction of bone. Documentation, including a cause of death of "pneumonic phthisis haemorrhage," and various biographic details exist for this burial. These suggest that B21's left and right midshaft femur were under asymmetric biomechanical and pathological conditions and should show differences in the underlying bone remodeling. *Methods:* We collected data on Haversian bone microstructure geometric properties and densities from a total of 148 secondary osteons and 481 Haversian canals. *Results:* The left femur, from the tuberculosis-inflicted hip joint, had fewer, larger, and more irregularly shaped canals and osteons than the right femur. *Discussion and Conclusion:* These findings may indicate the left femur received less biomechanical stimulation than the right femur due to decreased weightbearing. It is also possible that the tuberculosis infection in this individual impacted his bone metabolic activity, leading to increased experiences of bone loss. The presented histological approach may enhance interpretations in bioarchaeology by identifying whether bone remodeling changes occur as a result of long- or short-term disuse.

*Keywords:* histology; biomechanics; limb immobilization

Tkanka kostna jest dynamiczna i ulega przemianom metabolicznym w odpowiedzi na bodźce patologiczne i wynikające z aktywności fizycznej. Tę informację można odtworzyć w bioarcheologii metodami histologicznymi, które otwierają kolejną drogę do rekonstruowania życia przeszłych ludów. Raportujemy tutaj histologiczne wyniki z badań środkowej części kości udowej zidentyfikowanego osobnika z XIX wieku z Nowej Zelandii.

Received 03 March 2021

Revised 07 October 2021

Accepted 15 December 2021

Ten osobnik cierpiał na gruźlicę, która miała historycznie udokumentowane inwalidztwo. *Materiał:* Z miejsca pochówku 21 (B21) na Cmentarzu św. Jana w Milton wydobyty został szkielet mężczyzny w średnim wieku. Lewa bliższa kość udowa i kawałek kości miednicy wykazywały zmiany związane z destrukcją kości wywołaną efektem gruźlicy. Istnieje dokumentacja odnośnie tego osobnika, w tym przyczyna śmierci jako „krwotok płucny” oraz różne szczegóły biograficzne. Sugerują one, że lewa i prawa kość udowa w B21 były asymetryczne z perspektywy biomechanicznej i patologicznej. Te różnice powinny być odzwierciedlone w przebudowanej mikrostrukturze kości. *Metody:* Zebraliśmy dane dotyczące geometrii systemów Haversa badając właściwości i gęstości z łącznie 148 osteonów i 481 kanałów Haversa. *Wyniki:* Lewa kość udowa z dotkniętego gruźlicą stawu biodrowego miała mniej i większe kanały i osteony o nieregularnych kształtach niż prawa kość udowa. *Dyskusja i wnioski:* Te wyniki mogą wskazywać, że lewa kość udowa otrzymała mniejszą stymulację biomechaniczną niż prawa kość udowa z powodu zmniejszonego obciążenia. Możliwe jest również, że zakażenie gruźlicą w tym osobniku wpłynęło na jego aktywność metaboliczną kości, prowadząc do nasilenia doświadczeń związanych z utratą masy kostnej. Nasze wnioski mają implikacje metodologiczne i interpretacyjne dla prowadzenia ‘osteobiografii’ i wzmacniania modeli opieki w bioarcheologii.

*Keywords:* histologia; biomechanika; unieruchomienie kończyn

## Introduction

The reconstruction of human lives and lifestyles in bioarchaeology is traditionally achieved using macroscopic methods of skeletal examination, because they allow evaluation of anatomical variation in the light of behavioral and disease variables (Larsen 2015) and are noninvasive (Meyer 2011). However, bioarchaeologists increasingly recognize that using histological methods as a complementary tool of examination can yield microscopic data that offer insights into the underlying bone growth and change stimulated by various pathologies (Crowder and Stout 2011; De Boer and Van der Merwe 2011) and biomechanical load (Miszkievicz and Mahoney 2017; Stout et al. 2019), among other factors. In cases where permissions for destructive sampling of skeletal remains are in place, it is possible to extract small pieces of adult bone for examination under the microscope and measure geometric properties and densities of Haversian bone structures (secondary osteons, hereafter “osteons,” and Haversian canals) to reconstruct remodeling activity executed by bone multicellular units (BMUs) (Miszkievicz and Mahoney 2017; Stout et al. 2019). One application of such methodology in bioarchaeology can be seen in case studies that compare left and right limb bones’ microscopic changes in individuals afflicted with some form of unilateral condition, such as below-knee amputation (Lazenby and Pfeiffer 1993), hip joint ankylosis (Miszkievicz et al. 2020), or acute poliomyelitis-related lower limb atrophy (Kozłowski and Piontek 2000). Using archaeological and/or historical documentation evidence, the bone data can be contextualized to shed light on aspects of healing, care in the community, and experiences of short-term or long-term bone changes in past individuals.

## Cortical bone remodeling and unilateral limb pathology

Bone remodeling changes in cases of unilateral abnormalities can result from either biomechanical or pathological processes or their combined effect (Laroche et al. 2003; Ramírez et al. 2011). Although extrapolating one specific factor is difficult in nonexperimental (i.e., bioarchaeological) settings, broader interpretations within documented case studies can be conducted. Adult human cortical bone undergoes remodeling shifts with changes in biomechanical load (Augat and Schorlemmer 2006; Christen et al. 2014; Robling et al. 2006). Mechanical stimulation of bone tissue resulting in bone remodeling and modeling changes is described under Wolff’s law and the mechanostat theory (Frost 1998). Theoretical and experimental evidence indicates that bone tissue “rearrangement” occurs so that old bone is replaced with more structurally competent bone, or new bone is added at sites of high mechanical strain (Christen et al. 2014). Equally, limited or absent mechanical stimulus as a result of muscle disuse can lead to bone loss through an uncoupling of otherwise balanced remodeling activity of bone resorption and deposition (Alexandre and Vico 2011). The remodeling processes of secondary cortical bone can be reconstructed using geometric parameters of Haversian tissue seen in two-dimensional (2D) histology sections visualized using light microscopy (Stout et al. 2019). The shape and size of osteons, cortical bone remodeling products, reflect the stage and/or frequency of remodeling events (Hennig et al. 2015; Martin 2007).

Diseases that disrupt physiological homeostasis also systemically have the potential to disrupt an otherwise balanced bone remodeling, leading to bone loss dominating bone gain (e.g., Boyce et al. 2012; Walsh and Gravallesse 2010). This can be best illustrated

through osteopenia and osteoporosis, which are bone metabolic conditions characterized by increased bone fragility. While their etiology is complex, it also includes lack of biomechanical stimulation, as bone remodeling is disrupted for prolonged periods of time, such as in cases of bedrest or immobilization (e.g., Minaire et al. 1974; Schlecht et al. 2012). Infectious bacterial diseases, such as tuberculosis, which result in bone lesions including tuberculosis-induced hypertrophic osteopathy (Von Hunnius 2009) or local deposition of woven bone in response to the infection (Kuhn et al. 2007), can be examined alongside bone remodeling changes (Nair et al. 1996). One common manifestation of untreated tuberculosis infections is hip joint destruction (Babhulkar and Pande 2002), which is often one-sided and characterized by unilateral sclerotic lesions or acetabular migration (Vogelpoel et al. 2009). One-sided, tuberculosis-induced joint pathology will likely impact bone remodeling from both the disease and biomechanical viewpoint, as the afflicted individual does not have complete mobility of one leg (Babhulkar and Pande 2002).

The knowledge of modern-day presentation of remodeling changes in biomechanical and pathological contexts, combined with histology, offers a powerful means with which to test the extent that localized, cortical-bone mechanical adaptation occurs in archaeological cases of limb immobilization and disuse (e.g., Minaire et al. 1974; Schlecht et al. 2012). This histological approach may also enhance interpretations in bioarchaeology by identifying whether bone remodeling changes occurred as a result of long- or short-term disuse (Miszkievicz et al. 2020). For example, bone histomorphometry has been employed successfully in at least three previous bioarchaeological and paleopathological studies that address these sorts of questions (e.g., Kozłowski and Piontek 2000; Lazenby and Pfeiffer 1993; Miszkiewicz et al. 2020). Lazenby and Pfeiffer (1993) reported histologically informed endosteal expansion and increased cortical remodeling, along with macroscopic reduction in size of the left femur in a nineteenth-century Canadian (Middlesex County, Ontario) amputee. The individual had survived amputation approximately five years prior to death and was active following the application of the prosthesis. Kozłowski and Piontek (2000) used histology to show reduced bone density and osteocyte lacunae counts in the right metatarsal from a severely atrophic leg in a medieval (twelfth to fourteenth century A.D.) male from Gruczno, Poland. The authors suggest that this individual lived with a long-term, one-sided muscle paralysis caused by acute poliomyelitis. Most recently, Miszkiewicz et al. (2020) used bone

histology to report slight, midshaft femur remodeling asymmetry in a middle-aged male from Metal Period Nagsabaran (Philippines) who had suffered from left hip joint ankylosis. The bone remodeling changes were concluded to have been short term due to no severe (e.g., cortical trabecularization) bone resorption changes observed histologically. In all cases, the examined individuals would have experienced a form of biomechanical loading change to one side of their lower limbs.

#### Burial 21, Saint Johns, Milton

Following Captain James Cook's visits in the late eighteenth century, Aotearoa/New Zealand experienced several successive periods of immigration during the nineteenth century. One of the most significant agents of this migration was the New Zealand Company (NZC), which was formed in 1837 with the intention of profiting from the sale of land. The Otago settlement was a joint venture between the Lay Association of the Free Church of Scotland and the New Zealand Company, which purchased 144,600 acres of land in coastal Otago from Ngai Tahu (the local Maori tribe) in 1844. The intention was to establish a Wakefield class settlement, where the community would have two main social classes: a landowning capitalist class and a wage-earning working class (Hocken 1898:3; Olssen 1984:31–35; Schrader 2016:34–36). The head of Otago Harbour was selected as the site for the town, which was named "Dunedin," the Gaelic form of Edinburgh, and the first two immigrant ships arrived in 1848 (Hocken 1898:48, 57, 77–78, 81, 94; McDonald 1965:1–4). Growth of the new settlement was initially slow, but in 1861, the first of the major Otago gold rushes occurred inland at Gabriel's Gully, followed by the larger Dunstan Rush in 1862 (Olssen 1984; Salmon 1963). These events brought a massive influx of people and capital to Dunedin and Otago, and the population of the town rose from 2,262 in 1859 to 15,790 in 1864 (McDonald 1965:44, 51).

The rural village of Milton, located approximately 50 km southwest of Dunedin, was established in 1850 and functioned as an agricultural satellite community (Sumpter and Lewis 1949:5–10). Being approximately equidistant between Dunedin and the Lawrence goldfields, Milton was well placed to service both locations with goods. When the gold rush subsided, it also presented an attractive option for former miners to settle, and it remains the service center for the predominantly agricultural Tokomairiro area.

In 2016, an excavation of St. John's Anglican Burial Ground (SJM), Milton, was conducted at the request of the local community. This work had the joint

objectives of identifying “lost” graves and exploring the lives of colonial New Zealanders through bioarchaeological analysis of their remains (Petchev et al. 2017). Following public consultation, an archaeological authority (No. 2017/171) was granted for excavation by Heritage New Zealand, and a disinterment license (No. 2016/17) was obtained from the Ministry of Health. The remains recovered from this excavation are curated at the University of Otago, Department of Anatomy and will be repatriated to SJM once analyses are completed.

Recently, an integrated case study of disseminated, tuberculosis (TB)–induced, femoroacetabular joint changes in skeletal remains belonging to a middle-aged male (B21) from SJM was reported. This was a unique case study where access to death records, obituaries, and coffin plate information was possible, and archival research identified a period of invalidism impacting B21 for about a year prior to his death. Historical documentation shows that the remains of B21 belong to a 42-year-old man who was born in Mitcham, London, and immigrated to New Zealand via Hobart, Australia, following the discovery of gold in central Otago in 1861. After the rush subsided, he settled in rural community of Milton, supporting his wife and 11 children as a laborer. Sometime in 1872, he became too ill to work, and his family was supported by a charitable society to which he belonged (The Ancient Order of Foresters [AOF]). He died on July 5, 1873, and his cause of death is listed as “pneumonic phthisis haemorrhage.” It was found that B21 exhibited lesions that, along with his documented cause of death, strongly support a diagnosis of disseminated tuberculosis (Snoddy et al. 2020). These include extensive destruction of the trabecular bone in the proximal femur (Fig. 1) and remodeled destruction of the margins of the left acetabulum, as well as lytic endocranial cranial lesions. On the basis of the lesions of the hip, it was speculated that the one-sided hip joint pathology would have had an adverse effect on B21’s lower limb function (Snoddy et al. 2020:234); however, no direct data to test this assumption were available. These data would help validate the corroboration between the surviving bone and documented evidence and provide a methodological avenue for future bioarchaeological research examining cases of one-sided hip joint pathologies.

Assuming that B21 did not have full ambulatory use of his left leg, we hypothesize here that B21’s left and right midshaft femur will display localized asymmetry in biomechanically stimulated bone remodeling. Building upon the prior research (e.g., Kozłowski and Piontek 2000; Lazenby and Pfeiffer 1993; Miszkiewicz et al. 2020) and principles of bone functional adaptation and disease processes discussed above, we



**Figure 1.** Computed tomography scan (posterior view) of the left femur of B21 showing extensive destruction of the trabeculae in the head and trochanters (arrows)(reproduced with permission from Snoddy et al. 2020:228).

considered a series of bone remodeling scenarios in key types of lower limb (dis)use:

- *Functional and complete use of both lower limbs:* we expect no, comparable, or similar differences in the micro-characteristics (e.g., densities, shape, and size of osteons) of remodeled bone in a symmetrically sampled location on the left and right femur. These

might simply reflect natural variation and bilateral asymmetry (we use a 10% threshold—see *Materials and Methods*). As such, one can infer that no long-term (several years) or short-term (several months) bone remodeling change had occurred prior to death.

- *Long-term immobilization of both lower limbs*: we would also expect no, comparable, or similar differences in the micro-characteristics (e.g., densities, shape, and size of osteons) of remodeled bone in a symmetrically sampled location on the left and right femur. However, we should see evidence for osteopenia or osteoporosis-like changes in bone microstructure (“disuse osteoporosis”; Rolvien and Amling 2021), with extensive cortical bone porosity characterized with “giant” neighboring pores coalescing one into another, and enlarged osteon areas (Schlecht et al. 2012). In extreme cases, these can lead to a trabecularization effect where cortical bone resembles trabeculae compromising bone tissue (see Miskiewicz et al. 2021).
- *Long-term immobilization of one lower limb*: we would expect to see substantial differences in osteon densities, shape, and size, in addition to one leg bone showing evidence of osteoporosis-like or trabecularization effect (as per above point).
- *Short-term immobilization of one lower limb*: we expect bone histomorphometric differences to exist when comparing the left and the right side, but no abnormal porosity (osteoporosis or trabeculariza-

tion) would be detected. Bone remodeling changes would have only been short term and/or active at the time of death. This is because cortical bone remodeling activity takes several months (Robling et al. 2006), but much longer is required for ongoing resorption resulting in micro-porosity coalescing into trabecularization (Andreasen et al. 2020).

Given the documented short-term changes to B21’s behavior prior to death, we predict the left femur from the pathological joint will show histological indicators of prolonged bone resorption.

## Materials and Methods

Standard demographic methods indicate that B21 was a middle-aged (35–49 years old) male of  $163.9 \pm 3.87$  cm stature, which is consistent with documentary evidence (Snoddy et al. 2020:223). The skeletal remains were well preserved overall, although all long bones exhibited some fragmentation. This meant maximum length could not be measured in either femur. Only the left femur of B21 had been measured in situ using sliding calipers, and this field measurement was used in the aforementioned stature estimation. The postcranial skeleton was disarticulated due to displacement by water entering the coffin at some point after decomposition and prior to coffin collapse (Fig. 2a).

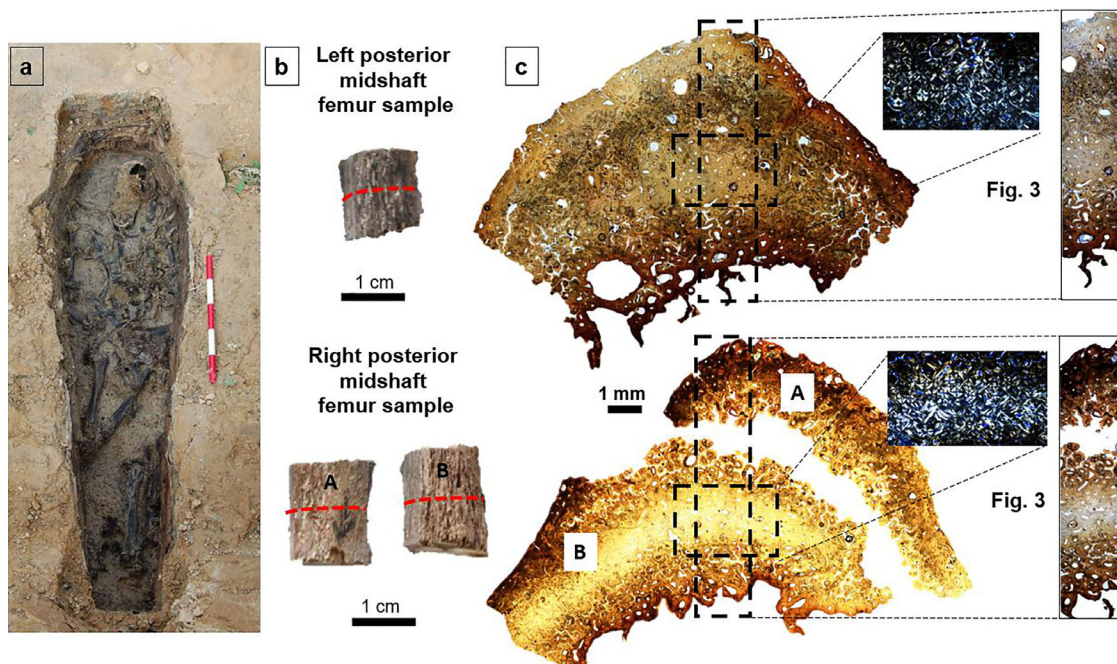


**Figure 2.** B21’s midshaft femur bone histology examined in the present study. The left (L) and right (R) femur are shown in (a) where the B21 burial is exposed (reproduced with permission from Snoddy et al. 2020). Panel (b) shows the femur samples postextraction where the red dashed line marks the cutting location for histology. Panel (c) shows overview bone histology for both the left and right femur samples, indicating (black dashed rectangles) regions of interest shown magnified in Figure 3 and the separated parts of the right sample (A and B).

Our sampling conduct followed ethical guidelines stipulated by Mays and colleagues (2013). Histology samples were extracted at the University of Otago anatomy laboratories, where the human remains are curated until the completion of the wider project this study is part of (Marsden Grant 18-UOO-028) and the repatriation of the remains. The histology samples were transferred to the Hard Tissue Histology laboratory in the School of Archaeology and Anthropology at the Australian National University, Canberra for histological expertise. The thin sections produced have been returned to New Zealand.

Small (approximately  $1 \times 2$  cm), cube-like cortical bone samples were extracted from the posterior midshaft of B21's left and right femur. The extraction occurred along the midpoint of the femoral midshaft overlapping the *linea aspera*, a muscularly important anatomical landmark (Goldman et al. 2009; Mittlmeier et al. 1994; Polguy et al. 2013), which captures localized bone remodeling in relation to mechanical stimulation (Miszekiewicz 2016). The midpoint of the *linea aspera* was identified following standard anatomical visual examination methods (e.g., Polguy et al. 2013). As the *linea aspera* extends over about a third of the total femur length, its proximal onset and distal ending along the femoral shaft can be easily determined visually. Its midpoint can then be estimated by subdividing the entire *linea aspera* length into equal segments (Polguy et al. 2013). A horizontal line measuring 2 cm and a vertical line measuring 1 cm were then marked with a pencil in preparation for extraction of cortical bone samples. Samples were cut using a standard Dremel 3000 130W tool equipped with a flex shaft direct-drive attachment and a 545 diamond-cutting wheel. Parallel transverse and longitudinal cuts were made following the pencil-marked lines so that each sample detached loosely (see technique described in Miszekiewicz and Mahoney 2016).

The preparation of thin sections followed standard methods (Miszekiewicz and Mahoney 2016, 2017) that involve embedding the samples epoxy resin (Buehler), cutting on a low-speed saw (Kemet MICRACUT 151 Precision Cutter), mounting on glass slides (using Stuk epoxy glue), grinding and polishing (on a Buehler EcoMet 300/AutoMet 300 Pro Touchscreen grinder-polisher), clearing in xylene, dehydrating in ethanol baths, and cover-slipping with DPX. Each section was approximately 100  $\mu\text{m}$  thick. The sample from the right femur broke into two smaller portions following the extraction. This happened while sectioning in a transverse plane, whereby the most posterior layer of bone separated from the more cortical portion. This was likely due to bone fragility underlined by the activity of postmortem taphonomic agents, which made the samples structurally brittle (Fig. 2b). However, the

impregnation with epoxy resin allowed us to contain both pieces for examination under the microscope. This meant we could not meaningfully measure the cortical width (in an anteroposterior plane) of each sample macroscopically (e.g., using digital calipers), so we had to use image analysis tools instead (see further below).

The sections were imaged using an Olympus BX53 microscope equipped with a DP74 camera at a total magnification  $\times 100$ . The entirety of each section was imaged first using the Olympus CellSens automatic stitching function (Fig. 2c). Qualitative analyses examining the section for presence of tissue abnormalities, such as trabecularization, were undertaken first. Quantitative analyses were then conducted. To ensure we examined "identical," in terms of size and relative position, regions of interest (ROIs) within each section, we captured a 9.02-mm<sup>2</sup> ROI intracortically by identifying a midpoint where arbitrary x and y axes cross when placed over each image (Figs. 2c and 3a,b).

Each of these ROIs showed well-preserved secondary osteons from which we could calculate standard bone histomorphometry variables that provide information about bone remodeling (Miszekiewicz and Mahoney 2016). These included osteon population density (OPD), which is a function of the number of intact and fragmentary secondary osteons divided by image area (in this case by 9.02 mm<sup>2</sup>), Haversian canal (H.Ar), osteon area (On.Ar) (in  $\mu\text{m}^2$ ), and osteon circularity (H.Cr, On.Cr) (Keenan et al. 2017; Miszekiewicz et al. 2020). Circularity is unitless and assessed on the scale of 0 to 1, with values of 1 indicating a "perfect circle" ( $\text{Cr} = 4\pi[\text{area}/\text{perimeter}^2]$ ; Keenan et al. 2017). In addition, we recorded a rectangular "strip" through the middle of each section so that subperiosteal bone was contained in each image (left strip area = 11.56 mm<sup>2</sup>, right strip area = 12.14 mm<sup>2</sup> excluding empty space). From this strip, we only measured H.Ar and H.Cr as cement lines of all osteons could not be consistently seen. However, we ensured we targeted the same number of canals in each sample, which was 143 (286 in total).

Additionally, we note that localized postmortem changes were apparent in the bone strips. For example, a distinct brown band of discoloration obscuring the periosteal and endosteal borders in each strip was visible (Figs. 2 and 3). This is in addition to orange staining along the entire length of the periosteal and endosteal borders and localized cracking when considering the full section. While histo-taphonomy is not the focus of our study, we note these changes are consistent with water damage (Pfretzschner 2004) and thus match the waterlogged environment of the B21 burial. Hollund et al. (2012) observed similar patterns in archaeological samples impacted by water damage,

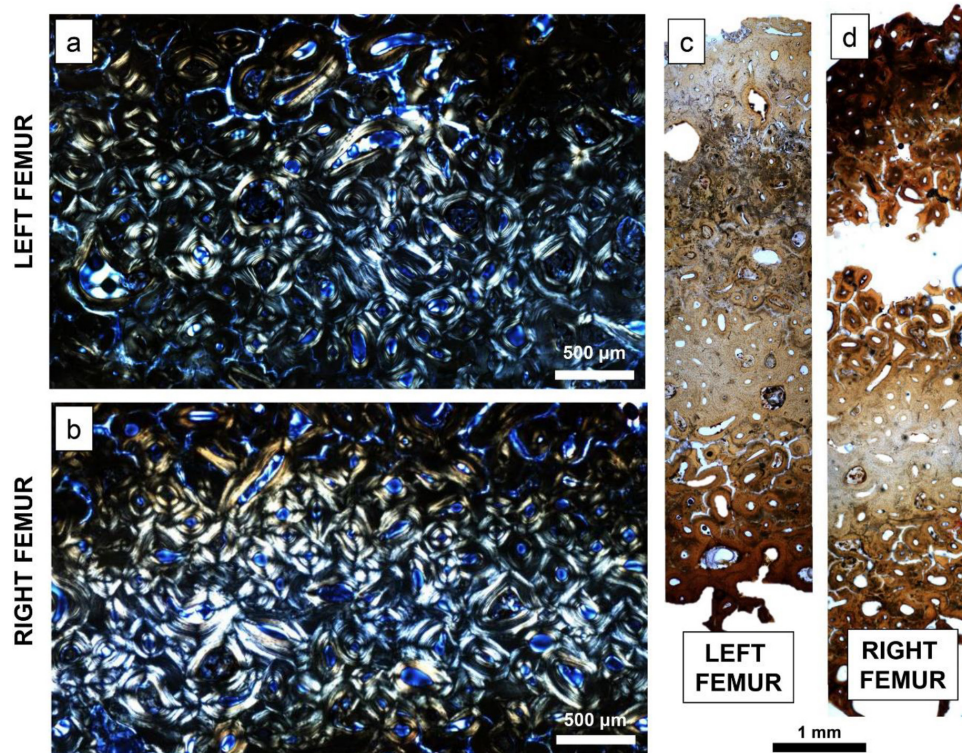


**Figure 3.** Regions of interest (ROIs) captured from each left and right femur cortical bone sample. The 9.02-mm<sup>2</sup> ROIs captured intracortically using linearly polarized light are shown in (a) and (b). “Longitudinal” strips of bone covering endosteal, intracortical, and periosteal bone regions are seen in (c) and (d). Please refer to Figure 2 to view the location of ROIs within their respective full scans of the samples.

where staining occurred along bone surfaces but deep cortical bone was protected, citing formation and oxidation of framboidal pyrite. Similarly, the intracortical bone in our samples is of almost pristine condition. The quality of archaeological bone histology preservation is traditionally assessed a 0 to 5 scale of the Oxford Histological Index (OHI; Hedges et al. 1995: 203), where 5 indicates almost modern-like bone (>95% of bone being intact). We assign 4 (>85%) to the full section, and 5 (>95%) to the intracortical ROI (see Figs. 2 and 3). To that end, we ensured that histology measurements were only collected from intact canals in the longitudinal strip (given inconsistent preservation of cement lines).

All the bone histology measurements were collected using the open access ImageJ/FIJI software (Doube et al. 2010) using the “freehand” tool for area measurements and the “multi point” tool for counts/density measurements. A minimum of 70 secondary osteons per section were examined, meeting recommended standards (25–50 osteons as per Stout and Crowder 2011). Cortical width of each sample measured from the most outer point on the endosteal to periosteal border was taken using the “straight line” function in ImageJ/FIJI, but it had to be combined from the two portions of the right sample. This introduces some

error, but we will treat this measurement cautiously in our interpretations, as it is the only insight into size differences between the left and right femur mid-shaft in B21. We report this value as an average of three repeated measurements. Comparisons of data between the left and right femur were undertaken on a descriptive basis, looking at measures of central tendency, given this is a case study. We report minimum, maximum, mean, and standard deviation (SD) data. Raw data generated in this study can be accessed from open access Figshare (Snoddy et al. 2021).

## Results

In terms of qualitative differences, when contrasting the left and right histology from each sample, there were no obvious abnormal or pathological malformations noted (see Table 1 for summary, Figs. 2 and 3). No significantly advanced bone resorption (e.g., evidence of cortical bone trabecularization) was observed in either of the samples. All bone present throughout the sections was densely remodeled Haversian tissue with several generations of osteons as inferred from fragmentary osteons widespread throughout each histology image (Figs. 2 and 3). No evidence of primary

**Table 1.** Summary of Qualitative Cortical Bone Histology Observations in Samples from B21.

Characteristic	Significance	B21
Cortical bone trabecularization effect originating on the endocortical bone and extending to the intracortical space.	Evidence for osteoporosis-like advanced bone resorption where pores coalesce into “giant” pores, which ultimately weaken bone quality and increase fragility (Chen et al. 2013).	No evidence for significantly advanced bone resorption noted, with all Haversian canals and osteons falling within typical parameters for humans. This confirms no long-term osteoporosis-like changes in bone quality.
Cortical bone tissue matrix presentation—primary and/or secondary Haversian tissue; woven and/or lamellar bone.	Primary bone indicates younger tissue (Goldman et al. 2009). Secondary bone indicates more mature tissue, which, if heavily remodeled, suggests older bone age (Jowsey 1960). Presence of woven bone would suggest active and rapid bone formation or healing, whereas lamellar bone lays down over longer periods of time (Shapiro and Wu 2019).	No woven and primary bone seen. Tissue is Haversian with multiple generations of secondary osteons, which confirms B21’s bone is well remodeled.
Histovariability in collagen fiber orientation osteon morphotypes.	Collagen fiber orientation can range from transverse (“light”) to longitudinal (“dark”) or be combined (“alternating”) (Bromage et al. 2003). Predominance of each type can suggest increased localized biomechanical loads of tension (longitudinal collagen—dark osteons) or compression (transverse collagen—light osteons) and/or a combination of loads (alternating osteons) (van Oers 2015).	Mostly alternating osteon morphotypes were observed reflecting a combination of collagen fiber orientation, which indicates no load-specific localized bone remodeling changes.
Multiple resorption bays spread throughout the bone cortex.	The presence of resorption cavities seen in cortical bone indicates bone resorption activated at the time of/just before death as an osteon formation had not had enough time to form (i.e., fill the cavity with new bone) (Goldman et al. 2009).	Left sample shows somewhat more resorption bays than the right, but it is difficult to account for histology “lost” to histo-diagenesis. Assuming left femur does have more bays, this could indicate more active resorption of bone when the left leg was not habitually loaded.

bone or simple primary vascularization of the cortex was observed either. No noticeable changes on the endosteal surfaces that would have been a result of non-taphonomic/diagenetic processes were apparent. Collagen fiber orientation throughout each sample showed no unusual patterning or clustering with a typical combination of light, dark, and alternating osteon morphotypes (Skedros et al. 2006). This suggests no specifically different localized mechanical changes in tension or compression (van Oers et al. 2015). In the left sample, there were somewhat more instances (at least 14) of active resorption cavities (evidence of osteoclast resorption with no refilling by osteoblasts in live bone; Goldman et al. 2009) within localized Haversian bone, but this was not substantially different from the right sample (at least 10). Because of the broken right sample, however, we cannot account for resorption cavities that might have been present in some of the missing cortical bone.

However, the quantitative analysis showed differences in histology between the left and right sample. Given the small sample size and data-violating assumptions for meaningful inferential statistical comparisons, our descriptive evaluations are based on prior studies comparing bilateral human femur anatomical, densitometric, and structural rigidity parameters using adult femora from cadavers (Pierre et al. 2010) and amputee patients (Åström and Stenström 2004; Finco and Menegaz 2021; Gholizadeh et al. 2019; Sherk et al. 2008). While Pierre et al. (2010) did not

specifically use histology to assess bone remodeling, they did report bone mineral density, which is a function of bone remodeling processes executed by osteoblasts and osteoclasts (Seibel 2002). Pierre et al. (2010) found that femoral side differences in macroscopic and densitometric parameters of less than 10% indicate natural asymmetry (e.g., Pierre et al. 2010), which corroborated prior findings in amputees (Åström and Stenström 2004; Finco and Menegaz 2021; Gholizadeh et al. 2019; Sherk et al. 2008). In the handful of prior studies implementing a similar research design to ours, bilateral bone histology differences to have arisen as a result of one-sided limb abnormalities either exceeded 10% (Lazenby and Pfeiffer 1993; Miskiewicz et al. 2020) or were quantified but not reported (Kozłowski and Piontek 2000). These studies used a range of cortical bone histology parameters to evaluate these changes, including percent remodeled bone (54% difference between left and right femur in Lazenby and Pfeiffer 1993), bone vascularity (31% difference between left and right femur in Miskiewicz et al. 2020), and osteocyte lacunae and trabecular bone density (“much lower” in an atrophied right metatarsal compared to a “healthy” metatarsal from the left side in Kozłowski and Piontek 2000:14). As such, we extrapolate the 10% figure to our study but acknowledge future bone histology research should attempt to validate this on larger archaeological samples.

In our study, all of the histomorphometric data measuring osteon densities and osteon and Haversian

canal size had lower mean values in the left sample when compared to the right (Table 2). This was the case using data both from the isolated intracortical ROI and the rectangular strips that overlapped endocortical and subperiosteal bone. However, using the aforementioned 10% difference as a threshold signifying normal versus abnormal bilateral difference, only the densities and area measurements of secondary osteons and Haversian canals, not the circularity values, were  $\geq 10\%$  different between the left and right

sample (Fig. 4, Table 2), with the Haversian canal area showing the largest difference (32%). This means fewer osteons of larger size had accumulated in the left femur compared to the right. Standard deviation data were also greater for the left H.Ar and On.Ar variables showing larger variability of osteon and canal size in the left sample. The circularity measurements of osteons and Haversian canals were descriptively higher in the right sample compared to the left, but they remained within a 10% difference (Table 2), with the

**Table 2.** Descriptive Data for All the Bone Histology Variables.

From 9.02 mm <sup>2</sup> Intracortical ROI											
Variable	N R	N L	Min R	Min L	Max R	Max L	Mean R	Mean L	%	SD R	SD L
OPD	120	107	n/a	n/a	n/a	n/a	52.426	37.650	<b>28</b>	n/a	n/a
On.Ar	70	78	10,670.485	7,915.970	115,781.647	155,948.723	36,446.247	40,446.481	10	20,009.108	27,973.641
H.Ar	100	95	598.924	1,122.056	46,574.946	87,017.520	7,020.628	8,692.155	<b>19</b>	7,416.530	13,464.385
H.Cr	100	95	0.403	0.250	0.982	0.987	0.894	0.873	2	0.103	0.131
On.Cr	70	78	0.758	0.598	0.983	0.980	0.934	0.920	1	0.042	0.062
From Full Midsection ROI Strip											
Variable	N R	N L	Min R	Min L	Max R	Max L	Mean R	Mean L	%	SD R	SD L
H.Ar	143	143	314.050	185.968	45,249.587	88,627.186	4,887.476	7,192.130	<b>32</b>	6,721.660	12,036.053
H.Cr	143	143	0.465	0.353	0.986	0.976	0.870	0.833	4	0.106	0.137

N, number of units; R, right; L, left; Min, minimum data; Max, maximum data; SD, standard deviation; ROI, region of interest; n/a, not applicable; OPD, osteon population density (number/ROI area in mm<sup>2</sup>); On.Ar, osteon area ( $\mu\text{m}^2$ ); H.Ar, Haversian canal area ( $\mu\text{m}^2$ ); H.Cr, Haversian canal circularity (unitless). Percent (%) values interpreted as abnormal difference are in bold.

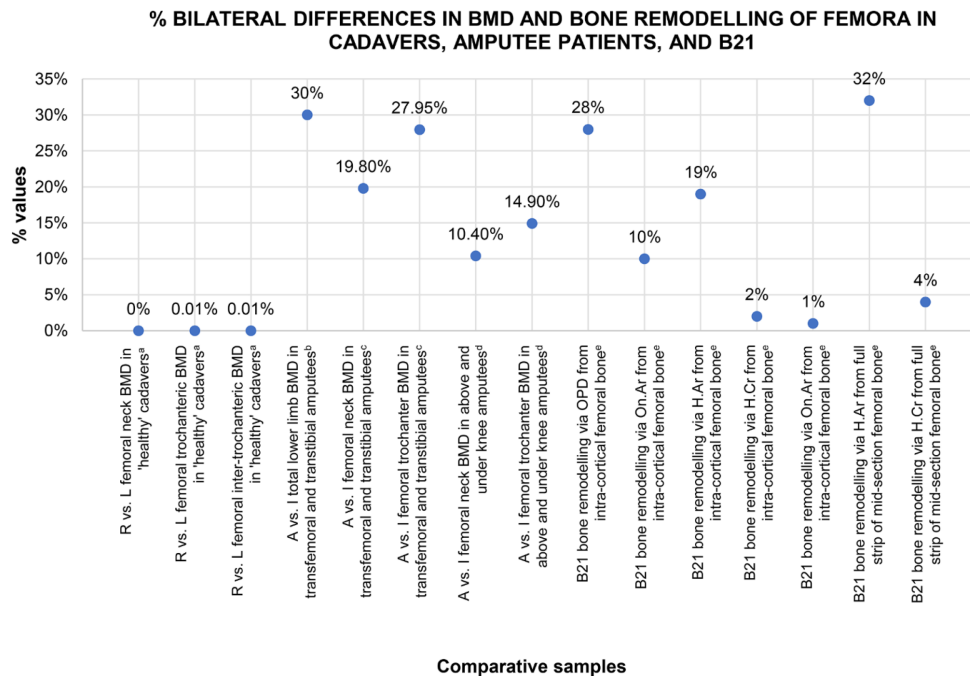


**Figure 4.** A simple plot illustrating where percent side difference in B21's proxy histology data for bone remodeling sits in comparison to percent side difference in bone mineral density (BMD, obtained via dual-energy X-ray absorptiometry) published data in naturally asymmetric femora from cadavers and amputee patients. R, right; L, left; A, amputated limb; I, intact limb; OPD, osteon population density (number/ROI area in mm<sup>2</sup>); On.Ar, osteon area ( $\mu\text{m}^2$ ); H.Ar, Haversian canal area ( $\mu\text{m}^2$ ); H.Cr, Haversian canal circularity (unitless). <sup>a</sup>Averaged data from  $n = 20$  cadavers in Pierre et al. (2010). <sup>b</sup>Averaged data from  $n = 4$  donors in Finco and Menegaz (2021). <sup>c</sup>Averaged data from  $n = 14$  amputees in Sherck et al. (2009). <sup>d</sup>Averaged data from  $n = 99$  amputees in Leclercq et al. (2003). <sup>e</sup>B21 data also reported in Table 2.

highest difference of 4% recorded for circularity of Haversian canals. This does mean the left femur had more irregularly shaped osteons and canals, but it is possible this is due to normal variation or both femora having circularity measures impacted by bone remodeling processes in a similar manner. The cortical bone width measured anteroposteriorly was slightly lower in the left sample (7.055 mm) when compared to the right (7.136 mm), but we need to treat this result cautiously given the fragmentation of the right sample.

## Discussion and Conclusion

In this study, we used histology to test whether localized bone remodeling differences between the left and right midshaft femur could be detected in an individual who had suffered from TB-induced, left-sided, femoroacetabular joint pathology. Our data for B21 suggest that his left midshaft femur had experienced short-term remodeling modifications likely lasting several months in the leadup to his death. The implications of these findings are discussed below.

### Burial 21's final illness: the histomorphometric evidence

The most plausible interpretation for the observed differences in midshaft femoral cortical microstructure is that the left femur experienced less mechanical load due to the macroscopically observed tuberculous destruction of the hip. This is because we did not observe any other microscopic changes (e.g., woven bone, trabecularized intracortex) in the left sample, except for the reported histomorphometric unilateral differences. However, we cannot exclude the possibility that a more generic/systemic disruption to the bone remodeling balance, resulting from the bacterial infection of B21, underlies the inferred increased bone resorption activity (Oliveira et al. 2020). It is known that lower limb mechanical load results in strain, which suppresses prolonged formation of larger secondary osteons (van Oers et al. 2008). Given the larger canals and osteons in B21's left femur, it is possible the increased load of the right leg was taken on by B21's right femur, where we see smaller, strain-suppressed, histostructures. Furthermore, because no "abnormal" bone porosity (i.e., where pores coalesce into larger pores and compromise cortical bone micro-architecture) was observed when comparing the left and right sample, a long-term bone remodeling change cannot be ascertained. Shorter-term bone remodeling alteration is more likely. Our finding matches the historical documentation that B21 was "invalid" for 11 months.

However, we should note that the destruction to this individual's left hip might have predated this, given that osseous TB is a chronic and slow progressing disease (Storm and Vlok 2009:495). As such, it is possible the individual's left leg might have been partially immobile before B21 stopped working. While some bacterial infections can have a localized effect on the skeleton, such as in the case of a tuberculosis-induced joint destruction, they can also dysregulate bone remodeling more systematically such that mineral deposition and bone resorption are out of balance (Oliveira et al. 2020). This could explain, alongside our biomechanical interpretation, why we see multiple BMUs created resorption cavities in both the left and right femur. Without experimental evidence, our discussion remains interpretative in nature.

Together, the findings align with the documented information about B21's inability to work for a year prior to his death (*Bruce Herald*, 11 February 1873). The ways in which this formed part of this individual's life experience remains unknown, but we show one biological aspect of his inability to work. The macroscopic lesions exhibited indicate the proximal portion of left femur was structurally compromised. However, the degree to which this affected his mobility is unclear. It would be inappropriate to attempt to reconstruct this individual's experience of impairment (see Battles 2009). The only documented information we have on this final period of B21's life is that he could no longer support his family through physical work and relied on the charity of the AOFs. Indeed, even the nature of his employment as a laborer is ambiguous, and we do not know what his work required other than that he be "able-bodied." At this time and place, he is most likely to have been employed either in building or farm work (possibly both), although Milton did also have a number of industries, including a flour mill and a brick and pipe works (the well-known local woolen mills and pottery works were both established after B21 died) (Sumpter and Lewis 1949:93–94). Whatever the exact nature of the laboring work, it would certainly been highly physical in this period.

### Histomorphometry: implications for the construction of osteobiographies

Our findings address the original speculation in Snoddy et al. (2020) that the limb function of B21 was restricted to some degree by the one-sided hip pathology. We add further to the biochemical and paleopathological analyses, combined with documented life history, by offering a more direct histological method of testing for individual-level localized bone functional adaptation in contexts of immobilization. This expands the bioarchaeology of care (Tilley 2015)

methodological toolkit, allowing bioarchaeologists to seek additional lines of data for inferences about instances of bedrest. The integrated case study for B21 included information on the lightness of his bones possibly indicating osteopenia (Snoddy et al. 2020:227). While our femoral histology data cannot diagnose this condition, they can clarify that B21's behavior and health were likely impacted prior to his death, which can be linked to poor systemic bone metabolism impacting calcium homeostasis. In their model of care, Snoddy et al. (2020) discuss how B21 would have required assistance with walking and mobility, which is supported by our histology data. As inferred from clinical literature (Babhulkar and Pande 2002), the tuberculous joint destruction in B21 would have likely caused significant pain and had a debilitating effect on his daily life, so we can also speculate periods of bedrest, impacting both femora. This could be tied to our histology data for the circularity measurements of osteons and Haversian canals, which did not differ substantially when compared between the left and right sample.

B21 provides another example of unilateral limb pathologies and associated bone histological changes reported in the paleopathological and bioarchaeological literature (e.g., Kozłowski and Piontek 2000; Lazenby and Pfeiffer 1993; Miskiewicz et al. 2020). As outlined in our introduction, these prior studies all reported such microscopic changes using skeletal remains from a range of time periods and geographical regions (medieval Poland, Metal Period Philippines, nineteenth-century Canada). All successfully determined asymmetric leg bone changes in remodeling reconstructed using the same histological measures of osteon densities (e.g., in Lazenby and Pfeiffer 1993) and circularity of Haversian canals (e.g., in Miskiewicz et al. 2020) as ours or similar measures of bone loss and gain, such as osteocyte densities approximating osteoblastic proliferation (Kozłowski and Piontek 2000). While Lazenby and Pfeiffer (1993) sampled the anterior femur, Kozłowski and Piontek (2000) examined the metatarsals, and Miskiewicz et al. (2020) sampled the posterior femur, as was the case in our study design, all found differences in bone histology. This suggests that histological methods are powerful enough to detect microscopic adaptation to load and pathological changes at the individual level. Because the recovery of human skeletal remains displaying such pathologies is rare, we believe that there is potential in ethical (e.g., removing small amounts of bone) histological sampling of limb bones to address questions that cannot be tackled using macroscopic methodologies alone.

It is worth noting that bone biology research using experimentally (un)loaded animal models (e.g.,

Jaworski et al. 1980; Young et al. 1986), living humans (e.g., Sibonga 2013), and postmortem human samples (Michael 2018; Schlecht et al. 2012; Stout 1982) has long provided evidence for limb disuse osteoporosis. Specifically, astronauts suspended in weightless environments are notorious for returning to Earth with severely advanced bone loss (Sibonga 2013), and immobilized Southern pig-tailed macaques (*Macaca nemestrina*) develop prolonged bone resorption over the initial seven months of mechanical unloading (Young et al. 1980). In light of the modern bone biology research, bioarchaeological and paleopathological cases studies, such as ours, can contribute historical data that conform to mechanical and bone physiological paradigms—forming a truly interdisciplinary approach to understanding the nature of bone tissue.

#### Limitations and future research directions

Because ours is a case study, there are a series of limitations that have hindered a more in-depth exploration of histology in B21. Given the poor preservation of long bones in this previously waterlogged burial, we could not obtain femur maximum lengths or robusticity measures from the femora to assess whether B21's left femur experienced modification (modeling) to its shape and size. We did, cautiously, note a slightly lower cortical width of the left sample when compared to the right. However, the magnitude of this (0.081 mm) difference is extremely unlikely to indicate modeling changes between the two femora. Comparisons of data in previous studies of similar research design noted differences on a much larger scale. For example, Lazenby and Pfeiffer (1993) reported a 13.8% difference in the midshaft anteroposterior diameter in the femora of the nineteenth-century Canadian amputee. Kozłowski and Piontek (2000) reported atrophied cortical width to measure 5 mm compared to 11 mm in a functional limb bone. The difference in B21 is only approximately 1.14%, which is very close to the 1.33% reported by Miskiewicz et al. (2020) for the same variable measured in the Metal Period Filipino individual's femora, where short-term remodeling changes were inferred. Furthermore, given the documented short-term invalidism in the year before B21's death, this would have not been enough time for macroscopic adaptation to develop in an adult femur. Cortical bone samples from the tibia would have allowed us to assess the distribution of histological features along with mechanical signal impacting the lower leg bones, but we did not have access to such samples. We did not have access to bone mineral density data either. These would have helped us confirm the suspected osteopenia and/or localized changes in calcium exchange at the midshaft femur. Finally, we have

identified that a large archaeological sample study is necessary in the future to validate how much of bone histology bilateral differences are due to natural asymmetry. Nevertheless, we have shown that bone histological analyses can complement multi-methodological examinations as part of osteobiographies conducted in bioarchaeology and bioarchaeology of care models.

It is clear that histological analysis of bone has a place in the study of disability and care in the past and, acknowledging that destructive analysis is not always possible, should be considered an integral part of the bioarchaeology tool kit. Nondestructive microscopic methods, including micro-computed tomography, should also be considered where possible. Future work accessing burials similar to ours might shed more light on the length of time impacting bone remodeling prior to death, in relation to specific disease conditions. For example, it would be worth assessing differences in localized femur bone remodeling changes across categories of arthritic, bacterial infection, metabolic, and developmental diseases manifesting in joints. These all have different spectra of pathogenesis that determine the extent of impact on bone remodeling. Once contextualized with documented or archaeological evidence, a series of examples can be created for bioarchaeologists to consult when hypothesizing about lifestyle and disease using fragmentarily documented or preserved human remains.

## Acknowledgments

We thank the descendants of B21 for allowing us to conduct this study and the members of TP 60 project for preserving the history of Tokomairiro/Milton. This work was funded by a Marsden Fund Grant awarded to HB and PP (18-UOO-028). Funding contributions toward technical work at the ANU histology laboratory were from the Australian Research Council Discovery Early Career Research Award (DE190100068 to JJM), the ANU College of Arts and Social Sciences, and the Australian Government Research Training Program (RTP) Scholarship (to KMC). We are grateful to the anonymous reviewers for their feedback on the earlier versions of this manuscript.

## References Cited

Åström, Ingrid, and Anders Stenström. 2004. Effect on gait and socket comfort in unilateral trans-tibial amputees after exchange to a polyurethane concept. *Prosthetics and Orthotics International* 28(1):28–36.

Alexandre, Christian, and Laurence Vico. 2011. Pathophysiology of bone loss in disuse osteoporosis. *Joint Bone Spine* 78(6): 572–576.

Andreasen, Christina M., Lydia P. Bakalova, Annemarie Brül, Ellen M. Hauge, Birgitte J. Kiil, Jean-Marie Delaisse, et al. 2020. The generation of enlarged eroded pores upon existing intracortical canals is a major contributor to endocortical trabecularization. *Bone* 130:115127.

Augat, Peter, and Sandra Schorlemmer. 2006. The role of cortical bone and its microstructure in bone strength. *Age and Ageing* 35(s2):ii27–ii31.

Babhulkar, Sushrut, and Sonali Pande. 2002. Tuberculosis of the hip. *Clinical Orthopaedics and Related Research* 398:93–99.

Battles, Heather T. 2009. Long bone bilateral asymmetry in the nineteenth-century Stirrup Court Cemetery collection from London, Ontario. *Nexus: The Canadian Student Journal of Anthropology* 21(1):1–15.

Boyce, Brendan F., Elizabeth Rosenberg, Anne E. de Papp, and Le T. Duong. 2012. The osteoclast, bone remodeling and treatment of metabolic bone disease. *European Journal of Clinical Investigation* 42(12):1332–1341.

Bromage, Timothy G., Haviva M. Goldman, Shannon C. McFarlin, Johanna Warshaw, Alan Boyde, and Christopher M. Riggs. 2003. Circularly polarized light standards for investigations of collagen fiber orientation in bone. *The Anatomical Record* 274(1): 157–168.

*Bruce Herald* (newspaper, Milton, NZ), Feb. 11, 1873.

Buckley, Hallie R., Phillip Roberts, Rebecca Kinaston, Peter Petchey, Charlotte King, Kate Domett, et al. 2020. Living and dying on the edge of the Empire: A bioarchaeological examination of Otago's early European settlers. *Journal of the Royal Society of New Zealand* 52(1):68–94. <http://doi.org/10.1080/03036758.2020.1837189>

Chen, Huayue, Xiangrong Zhou, Hiroshi Fujita, Onozuka Minoru, and Kin-Ya Kubo. 2013. Age-related changes in trabecular and cortical bone microstructure. *International Journal of Endocrinology* 2013:213234. DOI: 10.1155/2013/213234.

Christen, Patrik, Keita Ito, Rafea Ellouz, Stephanie Boutroy, Elisabeth Sornay-Rendu, Roland D. Chapurlat, et al. 2014. Bone remodeling in humans is load-driven but not lazy. *Nature Communications* 5(1):1–5.

De Boer, Hans H., and A. E. Lida Van der Merwe. 2016. Diagnostic dry bone histology in human paleopathology. *Clinical Anatomy* 29(7):831–843.

Doube, Michael, Michal M. Kłosowski, Ignacio Arganda-Carreras, Fabrice P. Cordelières, Robert P. Dougherty, Jonathan S. Jackson, et al. 2010. BoneJ: Free and extensible bone image analysis in ImageJ. *Bone* 47(6):1076–1079.

Frost, Harold M. 1998. From Wolff's law to the mechanostat: A new "face" of physiology. *Journal of Orthopaedic Science* 3(5): 282–286.

Finco, Malaka G., and Rachel A. Menegaz. 2021. Skeletal asymmetries in anatomical donors with lower-limb amputations. *PM & R: The Journal of Injury, Function, and Rehabilitation*. Advance online publication. <https://doi.org/10.1002/pmrj.12599>

Gholizadeh, Hossein, Edward D. Lemaire, Emily H. Sinitzki, David Nielen, and Paule Lebel. 2019. Transtibial amputee gait with the unity suspension system. *Disability and Rehabilitation: Assistive Technology* 15(3):350–356.

Goldman, Haviva M., Shannon C. McFarlin, David M. L. Cooper, C. David L. Thomas, and John G. Clement. 2009. Ontogenetic patterning of cortical bone microstructure and geometry at the human mid-shaft femur. *The Anatomical Record* 292(1):48–64.

Hedges, Robert E. M., Andrew R. Millard, and Alistair W. G. Pike. 1995. Measurements and relationships of diagenetic alteration of bone from three archaeological sites. *Journal of Archaeological Science* 22(2):201–209.

Hennig, Cheryl, C. David L. Thomas, John G. Clement, and David M. Cooper. 2015. Does 3D orientation account for variation in

- osteon morphology assessed by 2D histology? *Journal of Anatomy* 227(4):497–505.
- Hocken, Thomas M. 1898. *Contributions to the Early History of New Zealand*. (Settlement of Otago). Sampson, Low, Marston and Company, London.
- Hollund, Hege I., Miranda M. E. Jans, Matthew J. Collins, H. Kars, Ineke Joosten, and Saskia M. Kars. 2012. What happened here? Bone histology as a tool in decoding the postmortem histories of archaeological bone from Castricum, The Netherlands. *International Journal of Osteoarchaeology* 22(5):537–548.
- Jaworski, Z. F. G., Maria Liskova-Kiar, and Hans K. Uhthoff. 1980. Effect of long-term immobilisation on the pattern of bone loss in older dogs. *The Journal of Bone and Joint Surgery* 62:104–110.
- Jowsey, Jenifer. 1960. Age changes in human bone. *Clinical Orthopaedics and Related Research* 17:210–218.
- Keenan, Kendra E., Chad S. Mears, and John G. Skedros. 2017. Utility of osteon circularity for determining species and interpreting load history in primates and nonprimates. *American Journal of Physical Anthropology* 162(4):657–681. DOI: 10.1002/ajpa.23154.
- Kozłowski, Tomasz, and Janusz Piontek. 2000. A case of atrophy of bones of the right lower limb of a skeleton from a medieval (12th–14th centuries) burial ground in Gruczno, Poland. *Journal of Paleopathology* 12(1):5–16.
- Kuhn, Gisela A., M. Schultz, Ralph Müller, and Frank J. Rühli. 2007. Diagnostic value of micro-CT in comparison with histology in the qualitative assessment of historical human postcranial bone pathologies. *Homo* 58(2):97–115. DOI: 10.1016/j.jchb.2006.11.002.
- Laroche, Michel, L. Moulinier, Philippe Leger, D. Lefebvre, B. Mazières, and H. Boccalon. 2003. Bone mineral decrease in the leg with unilateral chronic occlusive arterial. *Clinical and Experimental Rheumatology* 21(1):103–106.
- Larsen, Clark S. 2015. *Bioarchaeology: Interpreting Behavior from the Human Skeleton*. Vol. 69. Cambridge University Press, Cambridge.
- Lazenby, Richard A., and Susan K. Pfeiffer. 1993. Effects of a nineteenth century below-knee amputation and prosthesis on femoral morphology. *International Journal of Osteoarchaeology* 3(1):19–28.
- Leclercq, Marie-Madeleine, O. Bonidan, E. Haaby, C. Pierrejean, and J. Sengler. 2003. Study of bone mass with dual energy x-ray absorptiometry in a population of 99 lower limb amputees. *Annales de readaptation et de médecine physique: revue scientifique de la Société française de reéducation fonctionnelle de readaptation et de médecine physique* 46(1):24–30.
- Martin, R. Bruce. 2007. Targeted bone remodeling involves BMU steering as well as activation. *Bone* 40(6):1574–1580.
- Mays, Simon, Joseph Elders, Louise Humphrey, William White, and Peter Marshall. 2013. *Science and the Dead: A Guideline for the Destructive Sampling of Archaeological Human Remains for Scientific Analysis*. English Heritage Publishing with the Advisory Panel on the Archaeology of Burials in England.
- Meyer, Christian, Nicole Nicklisch, Petra Held, Barbara Fritsch, and Kurt W. Alt. 2011. Tracing patterns of activity in the human skeleton: An overview of methods, problems, and limits of interpretation. *Homo* 62(3):202–217.
- Michael, Amy R. 2018. Histological estimation of age at death in amputated lower limbs: Issues of disuse, advanced age, and disease in the analysis of pathological bone. *Journal of Forensic and Legal Medicine* 53:58–61.
- Minaire, P., Pierre Meunier, C. Edouard, Jean-Pierre Bernard, P. Courpron, and J. Bourret. 1974. Quantitative histological data on disuse osteoporosis. *Calcified Tissue Research* 17(1):57–73. DOI: 10.1007/BF02547214.
- Miszkievicz, Justyna J. 2016. Investigating histomorphometric relationships at the human femoral midshaft in a biomechanical context. *Journal of Bone and Mineral Metabolism* 34(2):179–192. DOI: 10.1007/s00774-015-0652-8.
- Miszkievicz, Justyna J., and Patrick Mahoney. 2016. Ancient human bone microstructure in medieval England: Comparisons between two socio-economic groups. *The Anatomical Record* 299(1):42–59. DOI: 10.1002/ar.23285.
- Miszkievicz, Justyna J., and Patrick Mahoney. 2017. Human bone and dental histology in an archaeological context. In *Human Remains: Another Dimension*. Academic Press, London, pp. 29–43.
- Miszkievicz, Justyna J., Claire Rider, Shimona Kealy, Christina Vrahnas, Natalie A. Sims, Jitraporn Vongsvivut, et al. 2020. Asymmetric midshaft femur remodeling in an adult male with left sided hip joint ankylosis, Metal Period Nagsabaran, Philippines. *International Journal of Paleopathology* 31:14–22. DOI: 10.1016/j.ijpp.2020.07.003.
- Miszkievicz, Justyna J., Frédérique Valentin, Christina Vrahnas, Natalie A. Sims, Jitraporn Vongsvivut, Mark J. Tobin, et al. 2021. Bone loss markers in the earliest Pacific Islanders. *Scientific Reports* 11(1):1–16.
- Mittlmeier, Thomas, Claus Mattheck, and Florian Dietrich. 1994. Effects of mechanical loading on the profile of human femoral diaphyseal geometry. *Medical Engineering & Physics* 16(1):75–81.
- Nair, Sean P., Sajeda Meghji, Mike Wilson, K. Reddi, P. White, and Brian Henderson. 1996. Bacterially induced bone destruction: Mechanisms and misconceptions. *Infection and Immunity* 64(7):2371–2380. DOI: 10.1128/iai.64.7.2371-2380.1996.
- Oliveira, Tiago C., Maria S. Gomes, and Ana C. Gomes. 2020. The crossroads between infection and bone loss. *Microorganisms* 8(11):1765.
- Olsen, Erik. 1984. *A History of Otago*. John McIndoe, Dunedin.
- Petchey, Peter, Hallie Buckley, Rebecca Kinaston, and Baylee Smith. 2017. A nineteenth century settlers' graveyard: Preliminary report on the excavation of St. John's Cemetery, Back Road, Milton, Otago. *Archaeology in New Zealand* 60(1):20–31.
- Pfretzschner, Hans-Ulrich. 2004. Fossilization of Haversian bone in aquatic environments. *Comptes Rendus Palevol* 3(6–7):605–616.
- Pierre, Melissa A., David Zurakowski, Ara Nazarian, Diana A. Hauser-Kara, and Brian D. Snyder. 2010. Assessment of the bilateral asymmetry of human femurs based on physical, densitometric, and structural rigidity characteristics. *Journal of Biomechanics* 43(11):2228–2236.
- Polgaj, Michał, Katarzyna Bliźniewska, Kazimierz Jędrzejewski, Agata Majos, and Mirosław Topol. 2013. Morphological study of linea aspera variations—proposal of classification and sexual dimorphism. *Folia Morphologica* 72(1):72–77. DOI: 10.5603/fm.2013.0012
- Ramírez, Juan F., Jéscia A. Isaza, Isabela Mariaka, and Jaime A. Vélez. 2011. Analysis of bone demineralization due to the use of exoprosthesis by comparing Young's Modulus of the femur in unilateral transfemoral amputees. *Prosthetics and Orthotics International* 35(4):459–466. DOI: 10.1177/0309364611420478.
- Robling, Alexander G., Alesha B. Castillo, and Charles H. Turner. 2006. Biomechanical and molecular regulation of bone remodeling. *Annual Review of Biomedical Engineering* 8:455–498. DOI: 10.1146/annurev.bioeng.8.061505.095721.
- Rolvien, Tim, and Michael Amling. (2021). Disuse osteoporosis: Clinical and mechanistic insights. *Calcified Tissue International*. Advance online publication. DOI: 10.1007/s00223-021-00836-1.
- Schlecht, Stephen H., Deborrah C. Pinto, Amanda M. Agnew, and Sam D. Stout. 2012. Brief communication: The effects of disuse

- on the mechanical properties of bone: What unloading tells us about the adaptive nature of skeletal tissue. *American Journal of Physical Anthropology* 149(4):599–605. DOI: 10.1002/ajpa.22150.
- Sherk, Vanessa D., Michael G. Bemben, and Debra A. Bemben. 2008. BMD and bone geometry in transtibial and transfemoral amputees. *Journal of Bone and Mineral Research* 23(9):1449–1457. DOI: 10.1359/jbmr.080402.
- Seibel, Markus J. 2002. Nutrition and molecular markers of bone remodeling. *Current Opinion in Clinical Nutrition & Metabolic Care* 5(5):525–531.
- Schrader, Ben. 2016. *The Big Smoke: New Zealand Cities 1840–1920*. Bridget Williams Books, Wellington.
- Shapiro, Frederic, and Joy Y. Wu . 2019. Woven bone overview: Structural classification based on its integral role in developmental, repair and pathological bone formation throughout vertebrate groups. *European Cells & Materials* 38:137–167.
- Sibonga, Jean D. 2013. Spaceflight-induced bone loss: Is there an osteoporosis risk? *Current Osteoporosis Reports* 11(2):92–98. DOI: 10.1007/s11914-013-0136-5.
- Skedros, John G., Shaun D. Mendenhall, W. E. Anderson, K. E. Gubler, J. V. Hoopes, and S. M. Sorenson. 2006. Osteon phenotypic morphotypes: A new characteristic for interpreting bone quality in cortical bone. *Transactions of the Orthopaedic Research Society* 31:1600.
- Snoddy, Anne-Marie E., Hallie Buckley, Charlotte L. King, Rebecca L. Kinaston, Geoff Nowell, Darren R. Gröcke, et al. 2020. “Captain of all these men of death”: An integrated case study of tuberculosis in nineteenth-century Otago, New Zealand. *Bioarchaeology International* 3(4):217–237.
- Snoddy, Anne-Marie E., Justyna J. Miskiewicz, K. Cooke, Peter Petchey, and Hallie Buckley. 2021. Femur bone histomorphometry for ID #B21—Snoddy et al, last modified on May 10, 2021. <https://figshare.com/s/40e90e499063a6ece06f>.
- Storm, Martin, and Gert J. Vlok. 2009. Musculoskeletal and spinal tuberculosis in adults and children. In *Tuberculosis: A Comprehensive Clinical Reference*, edited by H. Simon Schaaf and Alimuddin Zumla. Saunders, Philadelphia, pp. 494–503.
- Stout, Sam D. 1982. The effects of long-term immobilization on the histomorphology of human cortical bone. *Calcified Tissue International* 34(1):337–342.
- Stout, Sam D., and Christian Crowder. 2011. Bone remodeling, histomorphology, and histomorphometry. In *Bone Histology: An Anthropological Perspective*, edited by Sam D. Stout and Christian Crowder. CRC Press, Boca Raton, FL, pp. 1–21.
- Stout, Sam D., Mary E. Cole, and Amanda M. Agnew. 2019. Histomorphology: Deciphering the metabolic record. In *Ortner's Identification of Pathological Conditions in Human Skeletal Remains*. 3rd ed. Academic Press, San Diego, CA, pp. 91–167. DOI: 10.1016/B978-0-12-809738-0.00006-5.
- Sumpter, D. J., and J. J. Lewis. 1949. *Faith and Toil, The Story of Tokomairiro* (Otago Centennial Historical Publications). Whitcombe, Clutha District.
- Tilley, Lorna. 2015. *Theory and Practice in the Bioarchaeology of Care*. Springer, Heidelberg.
- van Oers, René F. M., Ronald Ruimerman, Bert van Rietbergen, Peter A. J. Hilbers, and Rik Huiskes. 2008. Relating osteon diameter to strain. *Bone* 43(3):476–482.
- van Oers, René F. M., Hong Wang, and Rommel G. Bacabac. 2015. Osteocyte shape and mechanical loading. *Current Osteoporosis Reports* 13(2):61–66.
- Vogelpoel, Els E., Jurjen J. Been, and Arthur A. de Gast. 2009. Two-stage treatment of acetabular bone defect in tuberculosis of the hip by intended ankylosis followed by total hip arthroplasty: A case report. *Cases Journal* 2(1):1–5.
- von Hunnius, Tonya. 2009. Using microscopy to improve a diagnosis: An isolated case of tuberculosis-induced hypertrophic osteopathy in archaeological dog remains. *International Journal of Osteoarchaeology* 19(3):397–405.
- Walsh, Nicole C., and Ellen M. Gravallesse. 2010. Bone remodeling in rheumatic disease: A question of balance. *Immunological Reviews* 233(1):301–312. DOI: 10.1111/j.0105-2896.2009.00857.x.
- Young, D. R., W. J. Niklowitz, Raymond J. Brown, Webster S. S. Jee. 1986. Immobilization-associated osteoporosis in primates. *Bone* 7(2):109–117. DOI: 10.1016/8756-3282(86)90682-4.